

FiRework: Field Refinement Framework for Efficient Enhancement of Deformable Registration

Haiqiao Wang, Dong Ni, and Yi Wang✉

Smart Medical Imaging, Learning and Engineering (SMILE) Lab,
Medical UltraSound Image Computing (MUSIC) Lab,
School of Biomedical Engineering, Shenzhen University Medical School,
Shenzhen University, Shenzhen, China
onewang@szu.edu.cn

Abstract. Deformable image registration remains a fundamental task in clinical practice, yet solving registration problems involving complex deformations remains challenging. Current deep learning-based registration methods employ continuous deformation to model large deformations, which often suffer from accumulated registration errors and interpolation inaccuracies. Moreover, achieving satisfactory results with these frameworks typically requires a large number of cascade stages, demanding substantial computational resources. Therefore, we propose a novel approach, the field refinement framework (FiRework), tailored for unsupervised deformable registration, aiming to address these challenges. In FiRework, we redesign the continuous deformation framework to mitigate the aforementioned errors. Notably, our FiRework requires only one level of recursion during training and supports continuous inference, offering improved efficacy compared to continuous deformation frameworks. We conducted experiments on two brain MRI datasets, enhancing two existing deformable registration networks with FiRework. The experimental results demonstrate the superior performance of our proposed framework in deformable registration. *The code is publicly available at <https://github.com/ZAX130/FiRework>.*

Keywords: Deformable image registration · Deformation refinement · Continuous registration · Brain MRI · Deep learning.

1 Introduction

Deformable image registration is a crucial foundational task in clinical practice, providing aligned information to assist doctors in diagnosis and interventions. The purpose of registration is to estimate the desired deformation field that warps the moving image to align with the fixed image. While numerous methods have been proposed to address deformable registration, including traditional approaches [1, 2, 4, 18] and deep learning methods [3, 7], tackling complex deformations remains challenging.

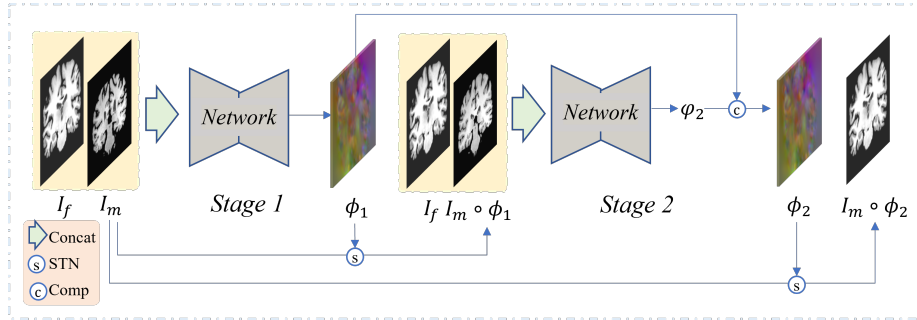


Fig. 1. Illustration of a two-stage continuous registration framework. I_f and I_m are the fixed and moving images, respectively. The network at stage 1 predicts the initial deformation field ϕ_1 . Then the warped moving image $I_m \circ \phi_1$, together with I_f , are sent into the network at stage 2 to compute the residual deformation field φ_2 . Finally, ϕ_1 and φ_2 are fused together to generate the overall deformation field ϕ_2 for registering.

To address this issue, recent studies relying on continuous deformation have been proposed [10,12,22–27]. These structures typically involve computing intermediate deformation fields to warp images or feature maps, followed by further residual field computation, and finally aggregating all fields to obtain the overall deformation field (see Fig. 1 for illustration). According to [25], the formula for obtaining ϕ_t from the deformation field ϕ_{t-1} is as follows:

$$\begin{aligned} \varphi_t &= f(I_m \circ \phi_{t-1}, I_f), \\ \phi_t &= \text{comp}(\phi_{t-1}, \varphi_t), \end{aligned} \quad (1)$$

where φ_t represents the residual subfield at step t , \circ represents the warping operation, typically performed by the spatial transformer network (STN) [11], f represents either a cascaded or recurrent network, with I_m and I_f being the moving and fixed images, respectively, and comp means the composition of continuous deformation field. If f in Equation (1) is a pyramid model, I_m and I_f represent the feature maps of a certain level for the moving and fixed images. However, such structures often encounter certain issues, such as the unavoidable impact of interpolation errors on feature extraction, as well as the influence of cumulative errors on the final deformation performance [27]. Moreover, multi-stage deformation structures often require cascading multiple deformation field generation networks during training [25], leading to increased network complexity and reduced training efficiency.

We have reconsidered the two types of error above. Firstly, we contend that relying solely on image information is insufficient to overcome the local minima induced by accumulated errors. This is primarily because the network lacks the knowledge of how I_m transforms to $I_m \circ \phi_{t-1}$ at stage t , thus unable to consider or address the origin of such errors, resulting in the forced convergence of $I_m \circ \phi_{t-1}$ towards I_f . Secondly, while interpolation errors might seem addressable by

directly inputting I_m , the objective of network is to compute φ_t on the basis of $I_m \circ \phi_{t-1}$, rendering the utility of I_m incomprehensible.

Recent attempts to address this problem by propagating semantic feature maps [16,23] or re-weighting multi-level deformation fields [6,15]. However, these approaches often lead to gradient explosion or substantial computational resource consumption.

In light of the challenges, we propose a novel field refinement framework (FiRework) for deformable registration networks. Unlike existing continuous deformation frameworks, our framework treats the network as a deformable field refiner. In this framework, we directly incorporate I_m and ϕ_{t-1} , as the relationship between I_m and $I_m \circ \phi_{t-1}$, into the network as extra inputs, allowing the network to reevaluate and optimize the previous deformation at each stage, thereby mitigating the issue of accumulated errors, and can leverage I_m to address interpolation errors. Moreover, our framework requires only a single-level recursion during training and allows for continuous refinement of the deformation field during inference, effectively reducing training costs and improving registration performance. The main contributions of our work are summarized as follows:

- We propose a novel deformable registration framework that bypasses interpolation and accumulation errors associated with continuous deformation by performing continuous deformation field refinement.
- The proposed framework entails a single-level recursion during training, while enabling multiple iterations for deformation field refinement during inference.
- We adapt two existing registration networks to the proposed framework, demonstrating substantial performance improvements in experimental results.

2 Method

2.1 Training Process

Our overall training process consists of two stages: the initialization stage and refinement stage, as illustrated in Fig. 2. Given the fixed image I_f and the moving image I_m , in the initialization stage, the network is modeled as follows:

$$\hat{\epsilon}_1 = f(I_m, I_m, I_f, \phi_{Init}), \quad (2)$$

where f denotes the network, ϕ_{Init} represents the initial deformation field initialized to zero, and $\hat{\epsilon}_1$ signifies the errors in the input deformation field. Thus, from the initialization stage, we obtain the first-stage deformation field ϕ_1 as:

$$\phi_1 = \phi_{Init} - \hat{\epsilon}_1 = -\hat{\epsilon}_1. \quad (3)$$

It is noteworthy that Equation (2) signifies that in the initialization stage, the network primarily relies on I_m and I_f to solve for the deformation field, which is

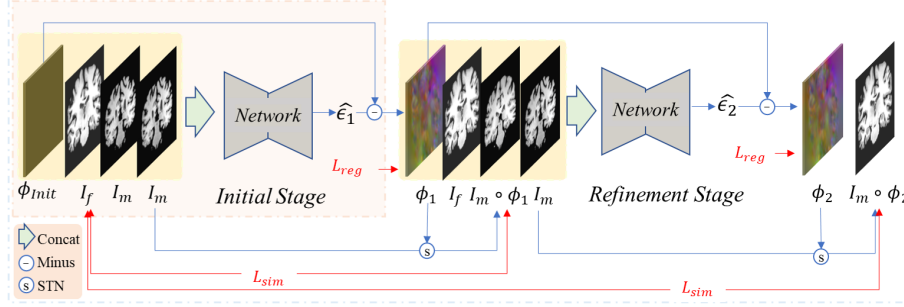


Fig. 2. Illustration of the training process of the proposed field refinement framework (FiRework). The training process is primarily divided into the initial stage and refinement stage.

consistent with the modeling of single-stage registration networks. We repeatedly input I_m in the initialization stage, and the input of the initial deformation field is primarily for consistency with the subsequent refinement stage. Through the initialization stage, we obtain a rough deformation field generated by the network.

To further improve the quality of the deformation field, we introduce a refinement stage. In the refinement stage, the network is modeled as follows:

$$\begin{aligned}\hat{\epsilon}_2 &= f(I_m, I_m \circ \phi_1, I_f, \phi_1), \\ \phi_2 &= \phi_1 - \hat{\epsilon}_2,\end{aligned}\quad (4)$$

where \circ is the warping operation and $I_m \circ \phi_1$ represents the image obtained by deforming the moving image using the first-stage deformation field ϕ_1 . During this process, the network learns the errors $\hat{\epsilon}_2$ in ϕ_1 based on the conditions $I_m, I_m \circ \phi_1, I_f$, and ϕ_1 , and subsequently eliminates it from ϕ_1 to derive the refined deformation field ϕ_2 . We design it to output $\hat{\epsilon}$ instead of directly providing the optimized deformation field in order to alleviate the workload of the network and enable it to utilize the input deformation field.

Because the network at stage t directly obtains refinement on ϕ_{t-1} , rather than the continuous deformation as in Equation (1), $I_m \circ \phi_{t-1}$ serves only as a reference, and the network focuses on learning how to better utilize the refined deformation field ϕ_t to directly deform I_m to I_f . Consequently, our proposed approach circumvents interpolation and accumulation errors inherent in continuous deformation frameworks.

To guide the learning process of the FiRework, our loss function is the sum of four losses as depicted in Fig. 2:

$$\mathcal{L} = \mathcal{L}_{\text{sim}}(I_m \circ \phi_1, I_f) + \lambda \mathcal{L}_{\text{reg}}(\phi_1) + \mathcal{L}_{\text{sim}}(I_m \circ \phi_2, I_f) + \lambda \mathcal{L}_{\text{reg}}(\phi_2), \quad (5)$$

where \mathcal{L}_{sim} represents the normalized cross correlation loss [17], \mathcal{L}_{reg} denotes the square of the gradient of the deformation field [3], and λ is the weight of the

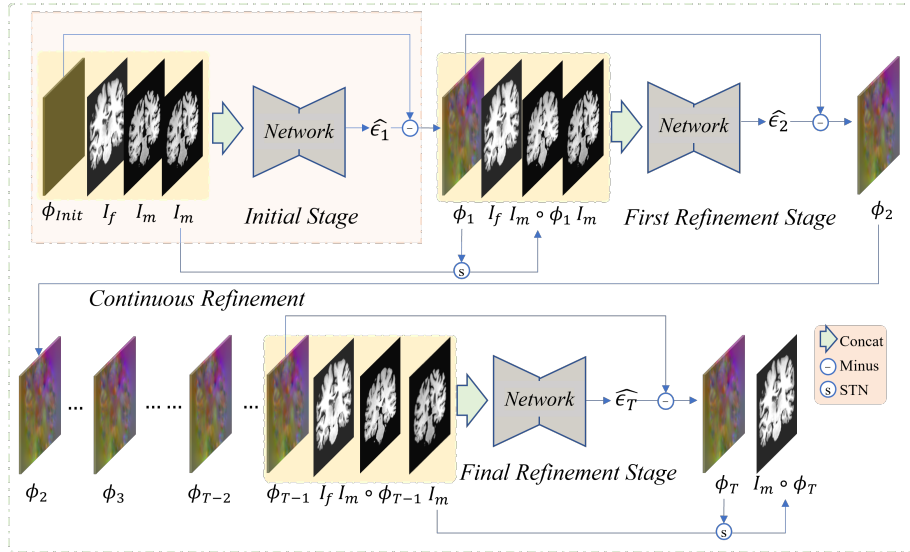


Fig. 3. Illustration of the inference process of the proposed FiRework. The figure illustrates the generation process from ϕ_1 to ϕ_T .

regularization term. It is important to note that the network in our framework shares parameters.

2.2 Inference Process

After training the network according to the aforementioned training process, we can obtain a network to directly optimize the coarse deformation field ϕ_t to obtain the refined deformation field ϕ_{t+1} , as illustrated in Fig. 3. During the initialization phase, we employ the same strategy as in the training process. Initially, we input $I_m, I_m, I_f, \phi_{init}$ into the network to obtain $\hat{\epsilon}_1$. Subsequently, we input $I_m, I_m \circ \phi_1, I_f, \phi_1$ to acquire $\hat{\epsilon}_2$, and iterate this process iteratively to obtain $\hat{\epsilon}_3, \dots, \hat{\epsilon}_T$. The final deformation field ϕ is then computed as:

$$\phi = \phi_T = - \sum_{t=1}^T \hat{\epsilon}_t. \quad (6)$$

Once the deformation field ϕ is acquired, the moving image I_m can be warped to obtain the registration result $I_m \circ \phi$.

3 Experiments

Datasets. Our experiments utilized two publicly accessible brain MRI datasets: LPBA [19] and Mindboggle [14]. The LPBA dataset comprises MRI volumes with

54 manually annotated regions of interest (ROIs). For training, we utilized 30 volumes (30×29 pairs), reserving 10 volumes (10×9 pairs) for testing. The Mindboggle dataset includes MRI volumes with 62 manually delineated ROIs. We combined the NKI-RS-22 and NKI-TRT-20 subsets to form the training set, comprising a total of 42 examples (42×41 pairs), and used 20 volumes from OASIS-TRT-20 (20×19 pairs) for testing. Pre-processing involved normalizing all voxel values to the range 0 to 1, and skull-stripping using FreeSurfer [9], resulting in volumes standardized to a final size of $160 \times 192 \times 160$ after center-cropping.

Evaluation Metrics. Quantitative assessment was conducted using Dice score (DSC) [8] as the primary metric, measuring the degree of overlap between corresponding regions. Additionally, the average symmetric surface distance (ASSD) [21] was computed to evaluate the similarity of surfaces. The quality of the predicted deformation field ϕ was evaluated by determining the percentage of voxels with a non-positive Jacobian determinant (i.e., folding ratio). All metrics were calculated in 3D space, with superior registration indicated by higher DSC, and smaller ASSD and folding ratio.

Comparison Methods. Our FiRework was compared against several state-of-the-art registration techniques: (1) SyN [1]: a classical traditional approach. (2) XMorpher (XM) [20]: a registration network incorporating cross-attention Transformer modules for each level of encoder and decoder. (3) VoxelMorph (VM) [3]: a classic one-stage registration network. (4) TransMorph (TM) [7]: a single-stage registration network with SwinTransformer enhanced encoder. (5) DMR [6]: a registration network using a Deformer and a multi-resolution refinement module. (6) PR++ [12]: a pyramid registration network using 3D correlation layer.

Implementation Details. Our methods included enhancing VM and TM with our FiRework, named FiRework-VM and FiRework-TM. The Adam optimizer [13] with a learning rate decay strategy was employed:

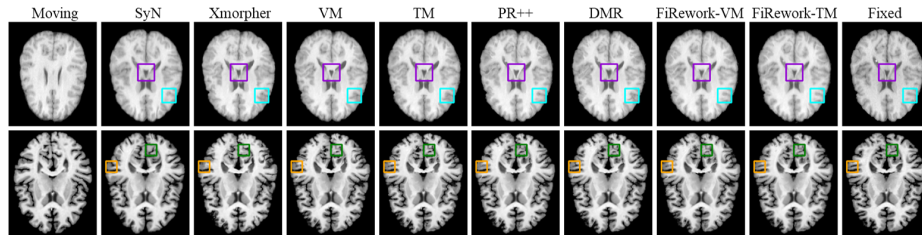
$$lr_m = lr_{init} \cdot \left(1 - \frac{m-1}{M}\right)^{0.9}, m = 1, 2, \dots, M, \quad (7)$$

where lr_m represents the learning rate of m -th epoch and lr_{init} represents the learning rate of initial epoch. For LPBA, we employed $lr_{init} = 0.0004$ and $\lambda = 4$. For Mindboggle, $lr_{init} = 0.0001$ and $\lambda = 1$. We set the batch size as 1, M as 30. The framework was implemented with PyTorch, using a GPU of NVIDIA RTX3090 with 24GB memory. We set T to 8 on LPBA and 5 on Mindboggle.

Quantitative and Qualitative Analysis. The quantitative results of different methods are reported in Table 1. FiRework-TM achieved the highest DSC and lowest ASSD on Mindboggle, 62.8% and 1.30mm, respectively, as well as the highest DSC on LPBA, while FiRework-VM obtained the lowest ASSD on

Table 1. The numerical results of different registration methods on two datasets.

	Mindboggle (62 ROIs)			LPBA (54 ROIs)		
	DSC (%)	ASSD (mm)	$\% J_\phi \leq 0$	DSC (%)	ASSD (mm)	$\% J_\phi \leq 0$
SyN [1]	56.7 ± 1.5	1.38 ± 0.09	$< 0.0001\%$	70.1 ± 6.2	1.72 ± 0.12	$< 0.002\%$
XM [20]	53.6 ± 1.5	1.46 ± 0.09	$< 0.2\%$	66.3 ± 2.0	1.92 ± 0.15	$< 0.1\%$
VM [3]	56.0 ± 1.6	1.49 ± 0.11	$< 0.2\%$	68.2 ± 2.3	1.84 ± 0.17	$< 0.004\%$
TM [7]	60.7 ± 1.5	1.35 ± 0.10	$< 0.2\%$	68.9 ± 2.4	1.82 ± 0.18	$< 0.02\%$
DMR [6]	60.6 ± 1.4	1.34 ± 0.09	$< 0.09\%$	69.2 ± 2.4	1.79 ± 0.18	$< 0.2\%$
PR++ [12]	61.1 ± 1.4	1.34 ± 0.10	$< 0.08\%$	69.5 ± 2.2	1.76 ± 0.17	$< 0.06\%$
FiRework-VM	60.0 ± 1.6	1.40 ± 0.10	$< 0.2\%$	70.4 ± 2.1	1.71 ± 0.15	$< 0.02\%$
FiRework-TM	62.8 ± 1.5	1.30 ± 0.10	$< 0.2\%$	70.5 ± 2.2	1.71 ± 0.17	$< 0.4\%$

**Fig. 4.** Registration results from different methods on LPBA (top row) and Mindboggle (bottom row).

LPBA. For the DSC results, FiRework-TM surpassed the second-best methods by 1.7% and 0.4% on Mindboggle and LPBA, respectively. On the LPBA dataset, FiRework-VM and FiRework-TM achieved 2.2% and 1.6% improvements compared to VM and TM, respectively. Moreover, on the Mindboggle dataset, FiRework-VM and FiRework-TM improved 4.0% and 2.1%. All these improvements were significant (Wilcoxon tests, $p < 0.05$). Table 1 also lists the percentage of voxels with non-positive Jacobian determinant ($\%|J_\phi| \leq 0$). Our method achieved acceptable performance.

Fig. 4 shows the registration results from different methods. Our method accurately registered corresponding structures. Fig. 5 illustrates the accuracy gains brought by each level of deformation in our FiRework. Fig. 6 takes the registration of one image pair as an example to show the refinement process of FiRework-TM. The final field ϕ_5 accurately warped the moving image to registered with the fixed image.

It is worth noting that compared to the original VM and TM, the FiRework-VM and FiRework-TM have increased their network parameters by only approximately 0.01 MB and 0.12 MB, respectively.

Analysis of Continuous Deformation Capability We compared our proposed framework with classical continuous deformation frameworks as shown in

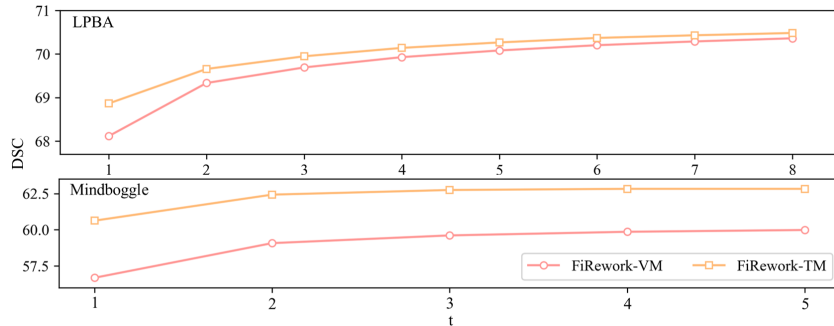


Fig. 5. Illustration of the DSC values obtained for each level of continuous deformation using the methods with proposed FiRework framework on two datasets.

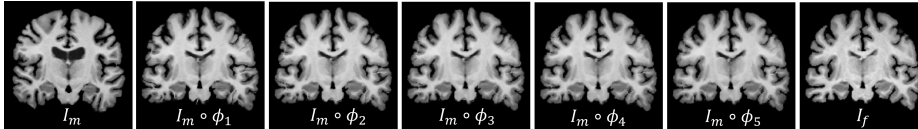


Fig. 6. Visualization of the refinement process using FiRework-TM for a single image pair from the Mindboggle dataset.

Fig. 7. Choosing VM with one recursion was because its training cost is similar to that of our framework. As shown in Fig. 7, VM reached its maximum value in the third round and then continued to decrease, mainly because the network did not know to continue cycling during learning and lacked the knowledge of how to further optimize near a local minimum point. Furthermore, VM-2 reached its peak performance at $t = 6$ and then remained relatively stable, mainly due to cumulative errors leading to deformation getting trapped in a local minimum, and interpolation errors causing the feature points on moving image to become blurred, making it difficult to achieve a better solution using this information alone. In contrast, FiRework-VM continuously optimized the deformation field and constantly referring to the original moving image, thus obtaining a better solution.

4 Discussion

We present a field refinement framework for the explicit optimization of the deformation field, where each stage takes into account the deformation field from the previous stage and predicts the errors present in the current stage’s deformation field. Furthermore, the proposed approach enables continuous optimization of the deformation field during the inference phase. Our primary motivation of the proposed FiRework is to leverage the network modeling the deficiency of the deformation field straightforwardly. This is different from almost all existing registration networks attempting to directly estimate the deformation field [3, 7, 28]

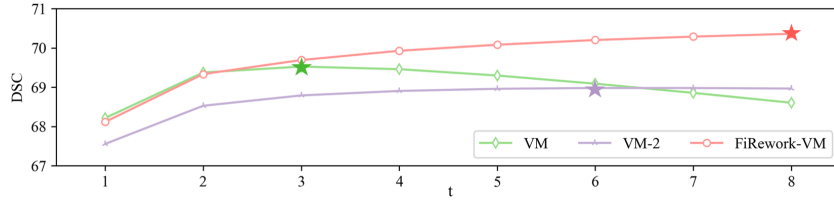


Fig. 7. Comparison of continuous deformation capability on the LPBA dataset with $T = 8$, measured by DSC. VM refers to VoxelMorph (VM) without recursive training and inference (Equation (1)). VM-2 denotes the VoxelMorph network trained and tested using the framework depicted in Fig. 1, with experimental setup consistent with our method. FiRework-VM represents our enhanced FiRework method. The asterisk symbol denotes the epoch with the maximum value attained.

or the residual subfield [5, 6, 12, 15, 20]. Compared to these existing methods, our proposed FiRework fully leverages the comprehensive information of the original image pair, the previous deformation field and its warped moving image, to refine the previous deformation field by analyzing its deficiency. We consider this as a more efficient solution. The efficacy of our FiRework on deformation field refinement can be observed from the quantitative and qualitative results in Table 1, Fig. 5 and Fig. 6.

Additionally, the proposed FiRework addresses the common issue in existing multi-stage registration methods, where cumulative errors and interpolation errors often degrade the registration performance. Our method effectively mitigates these issues, as demonstrated by its superiority shown in Fig. 7. The experimental results in Table 1 further illustrate that our FiRework can significantly enhance the performance of existing registration models (e.g., VM [3] and TM [7]) with minimal modifications, making it both a simple and highly effective solution.

Looking ahead, our current experiments have been limited to adapting existing networks to our FiRework. Therefore, future work may involve designing models that are more tailored to our framework. Additionally, our framework has not yet explored multi-resolution continuous deformation, an area we plan to explore in future research endeavors.

5 Conclusion

In this study, we introduce a novel field refinement framework (FiRework) for efficient enhancement of deformable registration. The proposed FiRework addresses the issues of error accumulation and interpolation in existing continuous deformation frameworks by directly optimizing the deformation field and re-inputting the moving image at each iteration. Our FiRework requires only one cycle during training, yet allows for multiple iterations during testing, efficiently enhancing the registration accuracy. Experimental evaluations were conducted

on two single-stage deformable registration networks using FiRework, and the results demonstrate the efficacy of our FiRework.

Acknowledgements

This work was supported in part by the National Natural Science Foundation of China under Grants 62471306 and 62071305, in part by the Guangdong-Hong Kong Joint Funding for Technology and Innovation under Grant 2023A0505010021, in part by the Shenzhen Medical Research Fund under Grand D2402010, and in part by the Guangdong Basic and Applied Basic Research Foundation under Grant 2022A1515011241.

References

1. Avants, B., Epstein, C., Grossman, M., Gee, J.: Symmetric diffeomorphic image registration with cross-correlation: Evaluating automated labeling of elderly and neurodegenerative brain. *Medical Image Analysis* **12**(1), 26–41 (2008)
2. Bajcsy, R., Kovačič, S.: Multiresolution elastic matching. *Computer Vision, Graphics, and Image Processing* **46**(1), 1–21 (1989)
3. Balakrishnan, G., Zhao, A., Sabuncu, M.R., Guttag, J., Dalca, A.V.: VoxelMorph: A learning framework for deformable medical image registration. *IEEE Transactions on Medical Imaging* **38**(8), 1788–1800 (2019)
4. Beg, M.F., Miller, M.I., Trounev, A., Younes, L.: Computing large deformation metric mappings via geodesic flows of diffeomorphisms. *International Journal of Computer Vision* **61**(2), 139–157 (2005)
5. Cao, Y., Zhu, Z., Rao, Y., Qin, C., Lin, D., Dou, Q., Ni, D., Wang, Y.: Edge-aware pyramidal deformable network for unsupervised registration of brain MR images. *Frontiers in Neuroscience* **14**, 620235 (2021)
6. Chen, J., Lu, D., Zhang, Y., Wei, D., Ning, M., Shi, X., Xu, Z., Zheng, Y.: Deformer: Towards displacement field learning for unsupervised medical image registration. In: *International Conference on Medical Image Computing and Computer Assisted Intervention (MICCAI)*. pp. 141–151 (2022)
7. Chen, J., Frey, E.C., He, Y., Segars, W.P., Li, Y., Du, Y.: TransMorph: Transformer for unsupervised medical image registration. *Medical Image Analysis* **82**, 102615 (2022)
8. Dice, L.R.: Measures of the amount of ecologic association between species. *Ecology* **26**(3), 297–302 (1945)
9. Fischl, B.: FreeSurfer. *NeuroImage* **62**(2), 774–781 (2012)
10. Hu, B., Zhou, S., Xiong, Z., Wu, F.: Recursive decomposition network for deformable image registration. *IEEE Journal of Biomedical and Health Informatics* **26**(10), 5130–5141 (2022)
11. Jaderberg, M., Simonyan, K., Zisserman, A., kavukcuoglu, k.: Spatial transformer networks. In: *Advances in Neural Information Processing Systems (NeurIPS)*. vol. 28 (2015)
12. Kang, M., Hu, X., Huang, W., Scott, M.R., Reyes, M.: Dual-stream pyramid registration network. *Medical Image Analysis* **78**, 102379 (2022)
13. Kingma, D.P., Ba, J.: Adam: A method for stochastic optimization. *arXiv preprint arXiv:1412.6980* (2014)

14. Klein, A., Tourville, J.: 101 labeled brain images and a consistent human cortical labeling protocol. *Frontiers in Neuroscience* **6**, 171 (2012)
15. Lv, J., Wang, Z., Shi, H., Zhang, H., Wang, S., Wang, Y., Li, Q.: Joint progressive and coarse-to-fine registration of brain MRI via deformation field integration and non-rigid feature fusion. *IEEE Transactions on Medical Imaging* **41**(10), 2788–2802 (2022)
16. Meng, M., Bi, L., Fulham, M., Feng, D., Kim, J.: Non-iterative coarse-to-fine transformer networks for joint affine and deformable image registration. In: *International Conference on Medical Image Computing and Computer-Assisted Intervention*. pp. 750–760. Springer (2023)
17. Rao, Y.R., Prathapani, N., Nagabhooshanam, E.: Application of normalized cross correlation to image registration. *International Journal of Research in Engineering and Technology* **3**(5), 12–16 (2014)
18. Rueckert, D., Sonoda, L.I., Hayes, C., Hill, D.L., Leach, M.O., Hawkes, D.J.: Non-rigid registration using free-form deformations: application to breast MR images. *IEEE Transactions on Medical Imaging* **18**(8), 712–721 (1999)
19. Shattuck, D.W., Mirza, M., Adisetiyo, V., Hojatkashani, C., Salamon, G., Narr, K.L., Poldrack, R.A., Bilder, R.M., Toga, A.W.: Construction of a 3D probabilistic atlas of human cortical structures. *NeuroImage* **39**(3), 1064–1080 (2008)
20. Shi, J., He, Y., Kong, Y., Coatrieux, J.L., Shu, H., Yang, G., Li, S.: Xmorpher: Full transformer for deformable medical image registration via cross attention. In: *International Conference on Medical Image Computing and Computer Assisted Intervention (MICCAI)*. pp. 217–226 (2022)
21. Taha, A.A., Hanbury, A.: Metrics for evaluating 3D medical image segmentation: analysis, selection, and tool. *BMC Medical Imaging* **15**(1), 1–28 (2015)
22. Wang, H., Ni, D., Wang, Y.: ModeT: Learning deformable image registration via motion decomposition transformer. In: *International Conference on Medical Image Computing and Computer Assisted Intervention (MICCAI)*. pp. 740–749 (2023)
23. Wang, H., Ni, D., Wang, Y.: Recursive deformable pyramid network for unsupervised medical image registration. *IEEE Transactions on Medical Imaging* **43**(6), 2229–2240 (2024)
24. Wang, H., Wang, Z., Ni, D., Wang, Y.: ModeTv2: GPU-accelerated motion decomposition transformer for pairwise optimization in medical image registration. arxiv preprint arxiv:2403.16526 (2024)
25. Zhao, S., Dong, Y., Chang, E.I.C., Xu, Y.: Recursive cascaded networks for unsupervised medical image registration. In: *International Conference on Computer Vision (ICCV)*. pp. 10600–10610 (2019)
26. Zheng, J.Q., Wang, Z., Huang, B., Vincent, T., Lim, N.H., Papież, B.W.: Recursive deformable image registration network with mutual attention. In: *Medical Image Understanding and Analysis*. pp. 75–86 (2022)
27. Zhu, Z., Cao, Y., Qin, C., Rao, Y., Lin, D., Dou, Q., Ni, D., Wang, Y.: Joint affine and deformable three-dimensional networks for brain MRI registration. *Medical Physics* **48**(3), 1182–1196 (2021)
28. Zhu, Z., Cao, Y., Qin, C., Rao, Y., Ni, D., Wang, Y.: Unsupervised 3D end-to-end deformable network for brain MRI registration. In: *2020 42nd Annual International Conference of the IEEE Engineering in Medicine & Biology Society (EMBC)*. pp. 1355–1359. IEEE (2020)